Title

Independent components of color natural scenes resemble V1 neurons in their spatial and color tuning

Journal

Journal of Neurophysiology, 91(6)

ISSN

0022-3077

Authors

Caywood, Matthew S
Willmore, Ben
Tolhurst, David J

Publication Date

2004

DOI

10.1152/jn.00775.2003

Peer reviewed

JN-00775-2003.R2

FINAL ACCEPTED VERSION

Independent Components of Color Natural Scenes Resemble V1 Neurons in their Spatial and Color Tuning

Matthew S. Caywood
Program in Neuroscience
University of California, San Francisco
San Francisco, CA 94143-0444, U.S.A.

Benjamin Willmore
Department of Psychology
3210 Tolman Hall #1650
University of California, Berkeley
Berkeley, CA 94720-1650, U.S.A.

David J. Tolhurst
Department of Physiology,
University of Cambridge,
Downing Street, Cambridge CB2 3EG, U.K.

Running Head: Color Tuning of Natural Scene ICs Resembles V1

Address for Correspondence:

Matthew Caywood
Department of Physiology
513 Parnassus Avenue, Room S-762
University of California, San Francisco
San Francisco, CA 94143-0444, U.S.A.
Tel: 415-476-1311 Fax: 415-476-4929
Email: caywood@phy.ucsf.edu

Abstract

It has been hypothesized that mammalian sensory systems are efficient because they reduce the redundancy of natural sensory input. If correct, this theory could unify our understanding of sensory coding; here, we test its predictions for color coding in the primate primary visual cortex (V1). We apply Independent Component Analysis (ICA) to simulated cone responses to natural scenes, obtaining a set of colored independent component (IC) filters that form a redundancy-reducing visual code. We compare IC filters with physiologically measured V1 neurons, and find great spatial similarity between IC filters and V1 simple cells. On cursory inspection, there is little chromatic similarity; however, we find that many apparent differences result from biases in the physiological measurements and ICA analysis. After correcting these biases, we find that the chromatic tuning of IC filters does indeed resemble the population of V1 neurons, supporting the redundancy-reduction hypothesis.

Introduction

The mammalian visual system is believed to efficiently encode natural visual information. One way in which it might do this is by reducing the redundancy of the representation at successive stages of processing (Attneave 1954; Barlow 1959). Natural visual input contains features such as edges and homogenous color patches, which make the patterns of light falling on the retina highly redundant and which give rise to statistical dependencies between neighboring regions of the visual image (Field 1987). In order to reduce redundancy, the visual system might use these features as a basis for representing visual input (Barlow 1989).

Independent Component Analysis (ICA, Comon 1994) is a widely used method for finding a redundancy-reducing encoding of data (such as natural visual scenes). Although the resulting “Independent Components” (ICs) are often only approximately independent, when ICA is applied to achromatic natural images, it produces ICs that are strikingly similar to the achromatic spatial receptive fields (RFs) of simple cells in primary visual cortex (V1) (Bell and Sejnowski 1997). Sparseness maximization (Olshausen and Field 1996) is conceptually similar to ICA and produces similar results; Ringach (2002) has argued that it better models the diversity of spatial RFs in V1. However, ICA has been validated by many rigorous comparisons with V1: van Hateren and van der Schaaf (1998) quantified the comparison between achromatic ICs and macaque V1 simple cells, and found that the distributions of all RF measurements except optimal spatial frequency (SF) were well matched. When a temporal dimension is added

and simple cells are compared to the IC filters of achromatic natural movies, the SF similarity improves (van Hateren and Ruderman 1998).

Since the ICA model successfully explains the spatial tuning of V1 simple cells to achromatic stimuli, the model may also explain other response properties such as color tuning. To test this hypothesis, ICA has been applied to colored natural scenes to produce spatiochromatic ICs (Tailor et al. 2000; Hoyer and Hyvärinen 2000; Wachtler et al. 2001; Doi et al. 2003). However, these studies used varying methodologies and found conflicting sets of ICs. Additionally, none of the studies has quantitatively compared ICs to a standard set of physiological measurements of V1. Finally, a richer understanding of V1 color coding has recently been developing: The view that color sensitivity is infrequent in V1 and restricted to weakly orientation-tuned neurons in cytochrome oxidase blobs (Livingstone and Hubel 1984; Lennie et al. 1990) has given way to a more diverse picture, in which oriented cells also have a rich variety of color sensitivities (Conway 2001; Johnson et al. 2001).

In this study, our goal was to rigorously test the hypothesis that ICA can account for the chromatic tuning of neurons in V1. We have controlled for the methodological variations between previous color ICA studies, and have chosen the most biologically realistic set of ICs for analysis. Treating the ICs as though they were real neuronal RFs, we use the cone-opponent grating stimuli of Derrington et al. (1984) to determine their color tuning. We then directly, quantitatively compare the color tuning with Lennie et al.'s (1990) classic V1 data. To further test the hypothesis, we compare the structure of ICs' model cone inputs with recent V1 data from Conway (2001) and Johnson et al. (2001). At first sight, the color tuning of ICs of natural scenes does not look very similar

to V1 neurons, but we will show that, in fact, there is considerable similarity, once appropriate ICA methodology is employed, and the limitations of real experimental protocols are considered.

Methods

Colored natural scenes

We analyzed a "hyperspectral" set of 25 distinct colored natural scenes (Párraga et al. 1998). Each 256x256-pixel scene was photographed through 31 filters covering the human visible spectrum (centered at wavelengths 400, 410…700 nm, bandwidth ~10 nm); thus it was not limited by the spectral sensitivity of a standard RGB camera. Each plane was digitized to 12 bits of intensity. We aligned the color planes of each scene with subpixel accuracy, by maximizing cross-correlation of adjacent planes; then, to ensure proper alignment, we averaged pixels together in 2x2 blocks.

We encoded the scenes in three ways that encompass previous work. Wachtler et al. (2001) transformed Párraga et al.'s hyperspectral images into the human visual colorspace defined by the absorption spectra of L, M and S cones. Hoyer and Hyvärinen (2000) used uncompressed images encoded in a digital camera's RGB colorspace, while Tailor et al. (2000) used JPEG-compressed RGB images taken from the Internet.

In the LMS condition, we used the Smith-Pokorny cone sensitivity curves (Figure 1e; Smith and Pokorny 1975) to transform the 31-plane hyperspectral scenes into 3-plane LMS space. These human psychophysical curves are consistent with, but more precise than, the physiological absorption spectra of macaque photoreceptors (Baylor et al. 1987). In the RGB condition, we converted the 31-plane hyperspectral scenes into 3-

plane RGB images, using the sensitivity curves (Figure 1f) of the red, green and blue detectors of a typical digital camera (Nikon Coolpix 950; C.A. Párraga, unpublished observations). In the JPEG condition, we applied JPEG compression to these RGB-encoded images, in order to mimic Tailor et al.'s dataset. JPEG images were encoded at quality setting 90 (using Matlab's (the MathWorks Inc.) IMWRITE function). This is conservative compared to the quality setting of between 50 and 75 which we estimate (from the encoded file sizes) was used in Tailor et al.'s image set. After performing ICA, we linearly transformed the resulting RGB ICs into the LMS colorspace for comparison with neurophysiological data.

We pseudorandomly extracted a set of 12x12-pixel fragments from the scenes in each image set, excluding the calibration reference (a white card) from each scene. The number of fragments was 200 times the fragment dimensionality (i.e. 86400 for 12x12-pixel, 3-plane images).

In the LMS and RGB conditions, each image fragment was log-transformed. The log transform is commonly applied as ICA preprocessing (e.g. van Hateren and van der Schaaf 1998) because it improves the convergence of ICA learning algorithms (see Willmore et al. 2000 for analysis of its effects). The raw luminance variation within our set of natural scenes, which covers three orders of magnitude, badly skews the data distribution and breaches the linear superposition model assumed by ICA (see next section). There are other remedies for this problem: while raw LMS images yield poorly converged ICs, standardizing the mean and variance of those images produces ICs similar to those of log-transformed images (data not shown). We chose to use the log transform, however, because it makes our results comparable with other studies.

From a functional point of view, the log transform has a clear biological correlate in retinal luminance adaptation (Field 1994, van Hateren and van der Schaaf 1998), a process which also compensates for the luminance changes (of many orders of magnitude) occurring in the natural environment. Our investigations of color tuning (below) are conducted in the equivalent of laboratory conditions, and always modulate cone contrast (at fixed mean luminance) rather than raw luminance. Therefore, we did not apply log transformation to our "grating stimuli."

In the JPEG condition, we did not apply the log transform, because our aim was to replicate the results of Tailor et al (2000), where the transform was not used.

Independent Component Analysis: algorithm and preprocessing

Each image fragment r_i was converted into a one-dimensional vector, and these comprised the rows of the 86400x432 data matrix R. The mean of each vector was set to zero. As a computational convenience for the ICA step, we whitened the data vectors; this transformation was inverted before the ICs were analyzed, so it has no effect on the final results. Our whitening method was based on Principal Components Analysis, and produced a data matrix $S = D^{-1/2}RE$, where the columns of E are the eigenvectors of the covariance matrix R^TR (i.e. its principal components) and D is a diagonal matrix containing the eigenvalues of the covariance matrix of R.

The assumption behind the ICA algorithm is that each image fragment x is composed of a weighted sum of a fixed set of underlying sources a_i whose activities are given by s_i:

$$x = \sum_{i=1}^{n} a_i s_i \qquad \text{or} \qquad x = As$$

These sources, also called basis functions, are identified as independent sources of variance of the image data, which produce image fragments by mixing together linearly. Along with the basis functions, one can also derive a set of IC filters which reverse the process: they "unmix" the image fragment to yield activity values s_i, which correspond to individual sources, and which should also be maximally independent. The set of filters produced by ICA is directly analogous to a population of V1 neurons, each analyzing part of the incoming visual stimulus.

There are a number of ICA algorithms, which make slightly different assumptions about the distribution of the underlying sources, but for ICA of colored natural scenes most algorithms yield similar results (Wachtler et al. 2001). We used an implementation of the information-maximization ICA algorithm with natural gradient feature (Bell and Sejnowski 1997, Makeig et al. 2002). This algorithm uses gradient ascent to find vectors in the distribution which give us the IC filter matrix F, which is the inverse of the sources: $F = A^{-1}$.

IC filters were similar over multiple runs of the algorithm, with different random seeds and different sets of image fragments. As a control for artifacts due to misalignment of the spectral planes, we performed extra analyses where we sub-sampled the LMS images in blocks of 2x2, 3x3 and 4x4 before extracting fragments; at each block size, the character of filters was preserved, which shows that the color planes were sufficiently aligned to prevent artifacts.

Spatial tuning

To find the best spatial stimulus for each IC, we exploited the equivalence between the Fourier transform of an RF and its responses to grating stimuli. We took the

two-dimensional discrete Fourier transform of each IC, identified the highest amplitude Fourier component, and computed its orientation and spatial frequency.

These measurements were limited in precision by the 12x12 patch size, because only discrete values corresponding to integer harmonics are possible. This patch size enabled us to measure orientation with precision of about 10 degrees, and to measure SF with precision of 1 octave at low SFs (near 0.1 cycles/pixel) and < 0.3 octaves at high SFs (near 0.5 cycles/pixel).

We also assessed other spatial properties of each IC. Using the best achromatic stimulus, we computed orientation bandwidth, SF bandwidth, length and width by measuring full width at half-maximum (FWHM) for bandpass functions, or twice the half width at half-maximum for low- and high-pass functions. SF bandwidth was computed as the log of the SF ratio between the half-heights in the amplitude spectrum along the radius corresponding to peak orientation, following van Hateren and van der Schaaf (1998). Orientation tuning bandwidth was measured as the difference between half-heights along the circle corresponding to peak SF. For a small number of very high-SF oblique filters, some measurements fell outside the boundary of the Fourier transformed patch; in these cases, we took the measurement at the boundary, which caused a slight narrowing of their bandwidth. Aspect ratio was computed as the ratio of the length and width, where the length is the RF envelope FWHM in the lowpass direction and width is the envelope FWHM in the bandpass direction (Field and Tolhurst 1986).

Color tuning

Color tuning was quantified using Lennie et al.'s (1990) cone-opponent stimuli in the "DKL" colorspace developed by Derrington et al. (1984) from the work of Macleod

and Boynton (1979). In this three-dimensional colorspace, the XY plane is equiluminant, similar to the CIE colorspace, and so any changes along the X and Y axes alter stimulus color without affecting luminance. Increasing *x* increases L-cone input while proportionally decreasing M-cone input (i.e. a stimulus becomes more "red" and less "green"), leaving S cones unaffected. Increasing *y* increases both L- and M-cone inputs while reducing S-cone input (resulting in more "yellow" and less "blue"). Increasing *z* increases input to all three cones, i.e. increases overall luminance. Lennie et al.'s white point was set to cone input values (0.311, 0.336, 0.353). Modulation from this point along the X axis to (1,0,0) corresponds to LMS cone input changes of (0.074, -0.14, 0), and modulation along the Y axis to (0,1,0) corresponds to changes of (0, 0, -0.84). Modulation along the Z axis causes a change in luminance without a change in color, so that modulation to (0,0,1) doubles all three cones' inputs. Because of the overlap of L and M cone spectra (Figure 1e), the effect of X axis modulation on L and M cones is small (compared to the effect of Y axis modulation on S cones) so we followed Lennie et al. in scaling the X coordinate by 3.125.

In the DKL colorspace, as defined in Lennie et al. (1990), a linearly summating neuron's color tuning can be described using only two parameters. To do this, we treat each set of coordinates (*x,y,z*) as a vector and describe it in spherical coordinates ($\varnothing,\theta,\rho$). The azimuth $\varnothing$ is the preferred color within the equiluminant XY plane: A neuron which is purely sensitive to R-G variation lies along the X axis and has an azimuth of 0°, whereas a neuron purely sensitive to B-Y variation lies along the Y axis and has an azimuth of 90°. The elevation θ is the angle the vector makes with the XY plane, and it describes the neuron's response to luminance change relative to chromatic change. A

neuron with elevation 0° responds best to chromatic stimuli, while a neuron with elevation 90° responds best to luminance stimuli. The stimuli are cone-opponent drifting gratings that are spatially modulated in color and luminance along the line defined by (ϕ,θ) and crossing the sphere defined by fixed ρ. Thus, a cell's color tuning can be fully described using only azimuth and elevations in the upper hemisphere ($\theta > 0^o$).

We computed the color tuning of each IC by finding the elevation and azimuth values that produce the maximal response, at a resolution of 1º. We converted each (ϕ,θ) pair into (x,y,z) coordinates and then converted these coordinates into cone-specific luminance values (L,M,S). To measure an IC's response to a color grating, we multiplied each cone luminance by the IC's Fourier component for that cone, summed the components over cones, and then took the amplitude.

Complementary to this cone-opponency analysis, we measured the cone-isolating grating responses of single cone inputs. In each color plane, we found the highest amplitude Fourier component and measured its phase, orientation, and SF.

Comparing color tuning distributions

The color tuning of each IC was thus represented by a single point in colorspace, $q(\phi,\theta)$. The distribution of all 432 ICs, $Q(\phi,\theta)$, was then compared with the distribution $P(\phi,\theta)$ of the 96 neurons described by Lennie et al. (1990). To compare two DKL color tuning distributions $P(\phi,\theta)$ and $Q(\phi,\theta)$, we needed a metric valid for arbitrary two-dimensional distributions. We used the Kullback-Leibler (K-L) distance from P to Q, which is also known as the relative entropy of P to Q:

$$\mathrm{D}(P\,||\,Q) = \sum_{\phi,\theta} P(\phi,\theta)\log\frac{P(\phi,\theta)}{Q(\phi,\theta)}$$

K-L distance is not symmetric, that is, in general $D(P||Q) \neq D(Q||P)$**.** However, when comparing physiological distributions $P(\phi,\theta)$ to IC distributions $Q(\phi,\theta)$, we avoid this issue by consistently using it in one direction $D(P||Q)$.

We binned the color tuning distribution into 30° x 30° bins, centered at azimuths -30°, 0° … 150° and elevations 15°, 45° and 75°. Some of the distributions had a small number n_0 of zero bins (oriented cells had 7, IC filters had between 1 and 4 depending on condition); to avoid singularity, these bins must be assigned a count. For each distribution, we wanted to calculate a zero-bin count which was as conservative (high) as possible. Therefore, we computed the maximum probability of data in each zero bin, p_0, such that the probability of no data falling in all n_0 observed zero bins was < 0.5 (since, in our single trial, we observed n_0 zero bins). The relative order of K-L distances was robust and our results did not change substantially for other bin sizes, center locations and zero bin counts between 0.01 and 1.

Measurements of K-L distance, like other information-theoretic measurements, cannot be assigned statistical confidence without extensive prior information. Therefore, these distances must be referenced to another distance value. We chose our reference to be the distance between Lennie et al.'s non-oriented and oriented cell distributions (shown in Figures 2c, 2d), which represents a substantial change between distributions, and is generally believed to represent a difference between cell classes. Because of the asymmetry of K-L distance, $D(\text{oriented} \,||\, \text{non-oriented}) = 0.97$ while $D(\text{non-oriented} \,||\, \text{oriented}) = 1.69$, so we took as our reference the average, 1.33. However, using either individual distance value does not affect our results.

Artifactuality in ICs

In our spatial and color tuning analyses, we considered the influence of artifactual ICs on the distribution of color tuning. Because ICA is a noisy optimization process with a finite data set, it will inevitably produce some artifactual ICs. However, using low variance as an indicator of artifactuality (as is commonly done) would introduce a bias against color, because color is a smaller source of variance in natural images than luminance (Ruderman et al. 1998). Therefore, we used van Hateren and van der Schaaf's (1998) criteria: artifactual ICs (1) extend over only a few pixels and (2) have nearly equal power in all four corners of the power spectrum. These criteria are entirely spatial and do not, a priori, introduce a color bias.

We also considered whether the limited size of image fragments could cause artifacts in the color tuning data. If spatial or spatial frequency edge effects were a problem, we would expect to see more artifactual bias at the smaller size. Notably, we obtained identical results using two patch sizes: 8x8 and 12x12 (data not shown). This suggests that edge effects do not significantly alter color tuning.

Spatial-chromatic separability assumption

We replicated Lennie et al.'s (1990) study of V1 neurons in two ways: (1) under ideal conditions, and (2) under conditions that imitate their exact methods, including experimental limitations. In the ideal case, we simultaneously measured spatial tuning (optimal orientation and SF) and color tuning (azimuth and elevation). In the imitation case, we followed Lennie et al.'s assumption that color and spatial tuning are separable (i.e. regardless of stimulus color, a cell will have the same optimal grating stimulus). Therefore, in this case we first measured spatial tuning using achromatic gratings, and

then used the orientation and SF of the best achromatic grating to make chromatic gratings for color tuning measurement. Lennie et al. sometimes re-optimized spatial tuning with a colored grating, and used colored gratings on occasions when achromatic ones did not work well. However, we excluded these heuristics, because they were not formalizable.

Effect of noise

A major difference between much modeling and real experiments is the presence of noise in the experiments. Therefore, when imitating Lennie et al.'s (1990) experiments, we tested the effect of noise on color tuning. We assumed that each IC's maximum amplitude of response modulation equaled 75 spikes per second, a value typical of Lennie et al.'s neuronal responses. For response modulations of that size, the amplitude standard deviation is approximately 5.25 spikes/s (Levine 1995). We simulated 25 different experiments, in which each grating stimulus was presented for 20 trials. To each trial's "grating response" (Fourier amplitude), we added amplitude noise with a standard deviation of 5.25 and a mean of zero. In each experiment, we averaged responses over all 20 trials and took the best stimulus as the color tuning. Then, to assess whether noise caused an overall bias, we computed the spherical mean of these color tuning measurements across 25 experiments (Fisher 1987).

Results

Starting with a set of hyperspectral images (Párraga et al. 1998), we constructed three different image sets with three color planes each (LMS-encoded, RGB-encoded, and JPEG-compressed RGB-encoded). We took each data set, performed Independent

Component Analysis, and obtained 432 IC basis functions and IC filters. Figures 1a-c show equivalent samples of ICA filters for the RGB, JPEG and LMS image sets, while Figure 1d shows a sample of LMS basis functions (see figure legend). Many of the filters look similar to the elongated Gabor function RFs of V1 simple cells (e.g. Ringach 2002), and many have apparent red-green (L-M) or blue-yellow (S-(L+M)) opponency. However, there are significant differences between the three sets of filters, in spatial structure and color tuning.

Figure 1 near here

JPEG Encoding Creates Artifacts in ICs

Both Tailor et al. (2000) and Hoyer and Hyvärinen (2000) have published ICA results from RGB images. Since Tailor et al.'s images were encoded using JPEG compression, which is lossy (i.e. does not preserve all information in the image), we investigated whether this had affected the ICs by directly comparing the effect of the different encodings on IC filters derived from our data set.

In the RGB condition, our IC filters (Figure 1a) corresponded fairly well to the basis functions of Hoyer and Hyvärinen, while in the JPEG condition, our filters (Figure 1b) were similar to those found by Tailor et al. We found that the spatial structure of the ICs found by Tailor et al. was indeed affected by JPEG compression of the source images: JPEG filters contained a large number of blue-yellow and red-green checkerboard patterns (e.g. rows 3-4, and 9-10 in Figure 1b) which do not correspond to any RGB filters. To ensure that these artifacts were the results of JPEG compression, and not the absence of the log transform, we also ran ICA on non-log-transformed RGB images. The

results (data not shown) are spatially similar to the log-transformed RGB ICs, not the JPEG ICs.

These artifacts result from JPEG's compression algorithm, which divides images into 8x8 blocks and then discards information within blocks. Because the image fragments used for ICA are not aligned with block boundaries, the boundaries become artifacts. JPEG encoding also produces chromatic artifacts, because it imitates an idealized human visual system by encoding images into luminance, red-green and blue-yellow color planes. Thus, ICA of JPEG images reveals mechanisms of the JPEG compression algorithm rather than features of the natural visual world.

RGB Encoding also Biases ICs

We next investigated the effect of using uncompressed RGB-encoded images, compared to the more biologically realistic LMS encoding. Hoyer and Hyvärinen (2000) justify their use of RGB images from a digital camera by arguing that the colorspace choice will make no difference. Because RGB and LMS colorspaces are related by a linear transform, they argue, the correlations in the data remain unchanged, thus ICA should produce the same ICs for both image sets. However, there are several nonlinearities in the digital camera's imaging process, such as color balancing and gamma correction, and preprocessing also includes another nonlinear step, the log transform. Because all of these nonlinearities may cause discrepancies between the RGB and LMS conditions, we decided to measure their influence on spatial and chromatic tuning.

The spatial structures of IC filters in the RGB condition (Figure 1a) and the LMS condition (Figure 1c) were very similar, insofar as both sets contain mostly elongated

Gabor-like features. There was noise in the LMS filters that was not present in the RGB filters, which was also true of the basis functions (data not shown). This may have resulted from the substantially greater overlap of L and M cone spectra (Figure 1e) compared to R and G detectors (Figure 1f): A given color image will have very similar L and M activations, and thus, image noise within the non-overlapping spectral regions will have an exaggerated effect on ICs in which L and M are opponent.

To compare color tuning in the RGB condition with the LMS condition, we linearly transformed RGB filters into the LMS colorspace, using the matrix of dot products between the RGB and LMS spectra in Figures 1f and 1e. Color tuning was summarized as the elevation (luminance sensitivity) and azimuth (chromatic preference) of the drifting sinusoidal grating that evoked the greatest response (see Methods). The color tuning of RGB filters (Figure 2a) differed substantially from LMS filters' color tuning (Figure 2b): RGB filters fell into a small number of line-like, continuous clusters corresponding to yellow (30° azimuth), magenta (135°), and blue (90°). LMS filters clustered at red (0°) and blue-magenta (120°), and were much more diffusely clustered. The shift in the centers of azimuth clusters suggests that the difference between RGB and LMS is not merely due to noise, and that, contrary to the claim of Hoyer and Hyvärinen (2000), RGB-encoded ICs are not appropriate after all for comparison with the visual system. Therefore, an ICA model of the visual cortex should use the visual system's LMS encoding of the chromatic information in natural scenes.

Insofar as RGB filters are comparable to the visual cortex, RGB encoding has one provisional advantage over LMS encoding: it reduces noise in the ICs, as explained

above. Consequently, although RGB encoding produces biased IC filters, any similarity to V1 cells actually supports our claim (below) that IC filters resemble V1 cells.

Figure 2 near here

LMS IC Filters have Similar Spatial Tuning to Simple Cells and Achromatic ICs

To examine whether color information affects the spatial structure of ICs, we compared the spatial properties of LMS IC filters with the spatial properties of achromatic IC filters (van Hateren and van der Schaaf 1998) and macaque simple cells (DeValois et al. 1982; Parker and Hawken 1988). We obtained the distributions of best orientation, orientation bandwidth, spatial frequency, spatial frequency bandwidth, and aspect ratio (envelope length divided by envelope width), using the best achromatic stimulus for each IC.

We identified artifactual ICs following van Hateren and van der Schaaf (1998)'s criteria; they constituted 29% (124/432) of our ICs. However, some of these artifactual ICs ad high variances (i.e. they were robust sources for the image data), so we also show, but do not discuss, spatial analyses for the full set of ICs.

The orientation distribution of non-artifactual filters (Figure 3a, gray bars) was similar to the distribution of achromatic filters, with peaks at 0º (vertical), 45º, 90º (horizontal) and 135º. The orientation bandwidth peak (Figure 3b, gray bars) was near 60º in our colored ICs, and the entire distribution seemed to be shifted towards higher values, compared to achromatic ICs and older studies of macaque V1 (DeValois et al. 1982; Parker and Hawken 1988), Interestingly, more recent physiological studies have reported an orientation tuning distribution much like ours (Ringach et al. 2002); in fact,

Ringach (2002) comments on the discrepancy between their data and achromatic ICA data, which is resolved by color ICA. The distribution of color filter spatial frequencies (Figure 3c) was qualitatively similar to achromatic filters, in that it increased exponentially with SF and peaked at the Nyquist frequencies for horizontal/vertical and diagonal filters. However, color filters were more diverse in preferred SF than achromatic, and better resemble the physiological data. The spatial frequency bandwidth distribution of color filters (Figure 3d) was similar to both achromatic filters (van Hateren and van der Schaaf 1998) and simple cells (DeValois et al. 1982). The aspect ratio distribution of color filters (Figure 3e) was centered at 1 (envelope length equal to envelope width), as with achromatic filters and simple cells (van Hateren and van der Schaaf 1998). Overall, with artifactual ICs removed, the distributions of the spatial parameters of colored IC filters were similar to the distributions reported for achromatic ICs, and fit the simple cell distributions about as well. The fit between the spatial properties of colored IC filters and simple cells was somewhat better for SF, marginally worse for aspect ratio, and while colored IC filters fit the most recent orientation tuning bandwidth data, achromatic IC filters fit the older data.

Figure 3 near here

LMS IC Filters, but not Basis Functions, have Similar Color Tuning to Oriented V1 Cells

Since LMS IC filters are spatially similar to simple cells, we compared the filters' color tuning with V1. We used the data of Lennie et al. (1990), who divided V1 cells into three classes: oriented, non-oriented and complex. We were primarily interested in the comparison with their oriented cells, which roughly correspond to simple cells, but since

many ICs are chromaticity sensitive we also considered non-oriented cells, which Lennie et al. found to be most color sensitive.

Comparing the color tuning of LMS filters (Figure 2b) to oriented V1 cells (Figure 2c), we found similar classes of color tuning in both. The azimuth distributions were bimodal, with a red-green (L-M) opponent cluster near 0° azimuth, and a slightly larger blue-yellow (S-(L+M)) opponent cluster near 90°. However, the azimuth distribution of chromaticity-tuned, S-cone sensitive filters was actually centered near 120°; thus, filters are closer to (S+L)-M cone opponency (135°). In both distributions, we found chromaticity-tuned and luminance-tuned RFs. Chromaticity-tuned RFs (at lower elevations) were bimodal, with very few intermediates. However, filters seemed substantially more chromaticity tuned than oriented V1 cells; a large number of L-M opponent filters with azimuths near 0° were purely chromatic, with elevations near 0°.

According to Lennie et al.'s (1990) strict criteria, which require a non-oriented cell to respond better to full-field modulation than to any grating, only one of our IC filters (a full-field noise patch) was non-oriented. Nevertheless, a moderately large population of filters had a center-surround-like organization reminiscent of blob cells (Livingstone and Hubel 1984), so we also compared the filters to Lennie et al.'s non-oriented (presumed blob) cells (Figure 2d). Like filters, non-oriented cells were basically bimodal in azimuth, with a red-green (L-M) cluster near 0° and a blue-yellow (S-(L+M)) cluster near 90°; however, the non-oriented cells' L-M mode was dominant, and azimuths between 30°-60° were more common. The elevation distributions of non-oriented cells and filters were similar: Both were bimodal, although non-oriented cells were less sharply so.

Previously, LMS IC basis functions (rather than LMS filters) have been compared to V1 (Hoyer and Hyvärinen 2000; Lee et al. 2002). Although there are a priori reasons why basis functions should not be analyzed this way (see Discussion), we have also observed that the color tuning of basis functions (Figure 2e) was markedly different from both V1 cells and filters: the distribution contained only a single cluster near azimuth 75° and elevation 75°. This is somewhat surprising, since basis functions are apparently diverse in color; however, their cone inputs were typically poorly balanced. Full-field luminance modulation, which is a poor stimulus for V1 cells, was the best stimulus for 73% of basis functions and <1% of filters; this empirically confirms that IC filters are the correct comparison for V1 cells.

Quantitative Comparison between IC Filters and V1 Shows Significant Similarity, once Experimental Biases are Removed

The color tuning of the LMS filters showed some qualitative similarities with Lennie et al's (1990) V1 cells; still, the raw filters contained two notably chromatic groups, near 0° and 120° azimuth, which were not strongly evident in the raw V1 data. However, comparing raw color tuning is misleading because it fails to take account of three discrepancies between the V1 data and the filters (see Methods). First, the raw ICA data included a subpopulation of artifactual low-variance ICs. Second, the V1 data assumed that spatial tuning can be determined achromatically before determining color tuning; that is, it assumes the best chromatic stimulus is spatially identical to the best luminance stimulus. This spatial-chromatic separability assumption might have biased measurements of color tuning. Third, the firing rates of V1 cells are subject to noise; this could also have biased estimates of cells' color tuning. Since we could not test the effects

of noise and separability on actual neurons, we measured their effects on the color tuning of the model IC filters.

Using van Hateren and van der Schaaf's criteria, we found that 29% of color ICs are artifactual, compared to the 25% of achromatic ICs they report. In terms of color tuning, these artifactual ICs (Figure 4a) tended to have very low elevations. Eliminating them made the color tuning of the remaining filters more similar to V1, in addition to improving spatial tuning.

To test what difference the spatial-chromatic separability assumption makes for our dataset, we compared chromatic tuning when spatial tuning was measured achromatically, with chromatic tuning when spatial and chromatic tuning were simultaneously determined. Measuring spatial tuning achromatically did bias color tuning. It caused elevations to increase and azimuths to decrease; that is, filters apparently became more luminance sensitive, and red-green opponency became more prominent (Figure 4b). Therefore, the physiological data's higher elevations, as well as its azimuth cluster at 90° rather than 120° (Figures 2c and 2d), may have been partly caused by this separability assumption.

Noise in neuronal responses is another possible source of bias. In Lennie et al.'s spherical coordinate system, there is a nonlinear relationship between elevation and stimulus contrast. In essence, because Z-axis modulation strength dominates the X and Y axes, cone contrast changes little with changes at low elevations, and much more with changes at medium elevations. For most cells, contrast determines the firing rate (and therefore noise level). Because noise increases with elevation, stimuli with higher

elevations are more likely to be experimentally misidentified as the optimal stimulus, which could cause a systematic upward elevation bias.

We measured the distance between the color tuning of noiseless IC filters and their mean color tuning with noise added, and found that noise biased the color tuning towards higher elevations (Figure 4c), causing a mean elevation overestimate of 7.6º and a number of severe (> 30°) overestimates. Thus, some of the higher elevations seen in the physiological data (Figures 2c and 2d) compared to the noiseless LMS IC filters (Figure 2b) may have arisen from noise in the physiological responses.

Thus, the assumption of spatial-chromatic separability, and the presence of noise in real V1 neuronal responses, both result in experimental biases that make cells appear dissimilar to IC filters. Furthermore, the inclusion of low-variance artifactual ICs in the comparison with real neurons also makes the IC filters look dissimilar to the real cells. Figure 4d shows how the color tuning of our IC filters (from Figure 2b) changes once we account for these three biases; it shows more similarity to the color tuning distributions of real V1 neurons (Figures 2c, 2d).

Figure 4 near here

To make the comparison between IC filters and V1 cells more rigorous, we measured the Kullback-Leibler (K-L) distance between the color tuning distribution of filters and the distributions of oriented cells (Figure 2c), non-oriented cells (Figure 2d), and both cell types combined (i.e. all non-complex V1 cells). K-L distances were normalized relative to a reference distance, which we took to be the distance between the distributions of oriented and non-oriented cells (see Methods).

We measured these normalized K-L distances for raw IC filters, filters corrected for each individual bias, filters corrected for noise and separability, and filters corrected for all three biases. While raw IC filters best resembled the pool of V1 cells, they were not especially similar to this group, or to the oriented or non-oriented groups, since all K-L distances were near 1 (Table 1, column 1). However, every single bias correction improved the fit between filters and all types of cells (Table 1, columns 2-4); correcting the noise bias had the largest effect. Noise and separability corrections appeared to be most important; subsequent to these, the effect of removing artifactual IC filters was only moderate (Table 1, column 5). When all three biases were taken into account (Table 1, column 6), the filters revealed a strong similarity to the pool of V1 cells, and substantial similarity to oriented and non-oriented cell groups.

Even after all biases were corrected, some residual differences between filters and V1 cells remained, contributing to the K-L distance. The low-elevation S-cone cluster fell at higher azimuths in filters than cells (120° rather than 90°), even after correction of the spatial-chromatic separability assumption. Also, there were non-oriented cells, but not filters, at intermediate azimuths (30-75°).

Ultimately, in all analyses of our filters, we found that the closest match (smallest K-L distance) was with the overall pool of V1 cells (Table 1, last row) rather than with any subpopulation, such as the more chromaticity-preferring non-oriented cells or the more Gabor-like oriented cells. It seems that IC filters are a heterogeneous group most similar in color tuning to the pool of oriented and non-oriented V1 cells.

Figure 5 near here

Dependence of Chromaticity on Orientation Selectivity is Consistent with Experimental Observations

Since it has been widely believed that responsiveness to purely chromatic stimuli is concentrated among non-oriented cells (Livingstone and Hubel 1984, Lennie et al. 1990), we examined the relation between orientation tuning bandwidth and chromaticity sensitivity (elevation in DKL space). Figure 5 shows that, indeed, filters with broad orientation tuning tend to be chromaticity sensitive and have low elevations. Filters with narrow orientation tuning are more diverse but have a tendency towards higher elevations. Non-artifactual filters are primarily responsible for this observation, since almost all artifactual filters have elevations near zero. Since most filters have relatively sharp orientation tuning, we can thus account for the physiological observation that non-oriented cells tend to be more chromatic, without assuming this implies that oriented cells are achromatic. In fact, our results are also consistent with Johnson et al.'s (2001) recent report that 79% of color-responsive neurons, stimulated with cone-isolating gratings (see below), had oriented RFs. Since most filters are well tuned for orientation, it emerges that most chromaticity-preferring filters do have fairly narrow orientation tuning.

Table 1 near here

Filters Fall into Two Strongly Double-Opponent Clusters

In order to compare ICs to another body of more recent physiological data (Conway 2001), we simulated the LMS IC filters' responses to cone-isolating stimuli. These stimuli avoid some of the confounds of cone-opponent stimuli, by modulating only one cone type at a time. For instance, in an L-cone isolating grating, the light stripe

increases L-cone excitation relative to background while the dark stripe decreases L-cone excitation. Although physiological cone-isolating measurements are often noisy and difficult to calibrate because of the overlap between cone absorption spectra (Conway 2001), in our model this measurement is trivial: we simply look at the filter's three color planes, which represent the individual LMS inputs.

For each IC filter, we measured its response amplitude to the optimal L, M, and S-isolating gratings, which indicates the relative strength of different cone inputs. We also measured its response phase to each grating, because this determines the spatial relationship between the cone inputs. For example, a cell could have L and M inputs with identical best orientation and SF, and if those inputs are in phase with each other (0° apart) the cell will be (L+M) or yellow sensitive. However, if they are 180° apart in phase, it will be L-M double-opponent. Figure 7a shows a schematic receptive field containing a double-opponent component (Michael 1978; Livingstone and Hubel 1984), which responds fairly specifically to a border between two colors (yellow and blue) because its inputs from the corresponding cones are opposite in sign.

Figure 6 near here

The response amplitude of all our IC filters to L, M, and S-isolating gratings of optimal orientation and SF is shown in Figure 6a (open circles). Filters fell into three clusters: One elongated cluster with high S response, some M response, and little L response; another elongated cluster with L and M response but little S response; and a diffuse cluster near zero. These roughly correspond to the azimuth modes of the cone-opponency data in Figure 2b.

To quantify the double-opponency of the different clusters, we compared the response phases of cone pairs. Among strongly L- and M- responsive filters (amplitudes > 100), L and M cones were almost always 180° apart in phase (94%, Figure 6b). Moreover, even though the optimal cone-isolating stimuli were not constrained by orientation and SF, 94% of L and M cone-isolating stimuli did have identical orientations and 95% did have identical SFs. Thus, for these double-opponent ICs, the spatiochromatic tuning to an L-cone-isolating stimulus predicts the tuning to the M-cone-isolating stimulus, which is consistent with Johnson et al.'s (2001) physiological measurements of SF.

Conway (2001) reported that, in a population of weakly oriented L-M cells studied with cone-isolating pixel stimuli, most S responses were in phase with M responses. These cells could therefore be called red-cyan (i.e. L-(M+S)). Among our L-M filters, the amplitude of S response indeed correlates with M response (lower cluster in Figure 6a), but the M and S inputs were phase opponent (Figure 6c) when measured at the M-isolating grating's best orientation and SF. Thus, our filters tend to show magenta-green ((L+S)-M) opponency, which was atypical but occasionally seen in Conway's data. This tendency of our filters may arise from the spectral overlap of M and S cones, which ICA will attempt to decorrelate even within L-M opponent IC filters.

Although there is little physiological data on S-cone double-opponency in V1, we measured its prevalence in our filters. Among S-responsive filters (S-isolating response amplitude > 20 units) we found double-opponency between M and S when measured at the S-isolating grating's best orientation and SF (Figure 6d). We might have expected that these S-cone driven filters would be opponent to yellow (L+M). However, in the

majority of filters, L and S actually have similar phase (Figure 6e), while the remainder are phase opponent. This is probably also due to the spectral overlap described above. Thus, our strongly S-responsive filters are also mostly magenta-green opponent, although a few are red-cyan. This prediction of our model has not yet been explicitly tested, although it does appear consistent with Lennie et al.'s data.

Figure 7 near here

Discussion

The colored IC filters of LMS-encoded natural scenes are similar to primate V1 cells in their color tuning, and are spatially similar to both simple cell receptive fields and achromatic ICs. This is a surprising result, given that V1 cells have often been reported to be mostly achromatic, especially those with oriented receptive fields (Hubel and Wiesel 1968; Livingstone and Hubel 1984; Lennie et al. 1990), whereas ICs have been reported to be unbiologically chromatic and double-opponent (Tailor et al. 2000). However, it emerges naturally from a biologically realistic set of LMS IC filters, when care is taken with the ICA methodology in order to make proper comparisons between V1 cells and ICA output, and when the reality of physiological experiments (such as response noise) is taken into account.

It is methodologically essential to use LMS encoding of natural scenes (as was also done by Wachtler et al 2001, Lee et al. 2002, and Doi et al. 2003); this accurately represents the chromatic information available to the cortical, experience-dependent stages of the visual system. Colored images encoded in the usual ways for transmission over, say, the internet (RGB or even JPEG encoding) produce filters that are not

appropriate for comparison; moreover, they are unlike real cells. Additionally, it is important to compare IC filters, not basis functions, with the physiological data. Although some previous studies (Hoyer and Hyvärinen 2000, Lee et al. 2002) have focused on basis functions, there is no theoretical justification for this (see below); additionally, we find that basis functions are dominated by properties (such as their strong response to full-field illumination) that have no counterpart in visual neurons.

The other major factor in this comparison is the correction of biases both in the IC analysis and the physiological data. A simplistic, uncorrected comparison between the IC filters and V1 cells (Lennie et al. 1990) suggests only a weak similarity (figures 2b and 2c). The ICs appear to be more chromatically tuned than the real neurons. However, we find that this comparison is skewed by several biases. Some of the IC filters are highly chromatic noisy structures; when these are eliminated, the remaining filters better resemble simple cells, spatially and chromatically. Similarly, we estimate that Lennie et al's V1 data are biased by their assumption of spatial-chromatic separability and by the effect of cortical noise.

Cortical noise is a particularly important source of bias in the Lennie et al physiological data. We find that, in a simulated neurophysiological experiment, achromatic (high-elevation) stimuli, which modulate all cones in concert, tend to produce noisier responses than chromatic (low-elevation) stimuli, which modulate contrast between two cone types. This skews measurements of color tuning, so that even cells' averaged responses make them appear much less chromaticity-sensitive than they actually are. Any method of finding the best color direction will be swayed by this noise, especially if it interpolates between (as do many experiments) or picks the best stimulus

(as does our simulation). Johnson et al. (2001) speculate that one reason for the lack of chromaticity-tuned cells in Lennie et al.'s study is that their stimuli only weakly modulate chromatic neurons. For modulation strength to directly influence tuning in the DKL colorspace, however, a nonlinearity is necessary; we suggest that noise is a very significant source of nonlinearity.

Analysis of these biases suggests that simple cells, which are generally not considered the substrate for color coding, are in fact more chromatically sensitive than has often been depicted. This result is independent of the correctness of our model, and aids in reconciling Lennie et al.'s study with a growing body of recent neurophysiology (Johnson et al 2001, Conway 2001).

The similarity between IC filters and V1 cells suggests that chromatic and spatial information are distributed across cells in V1 in a way that is compatible with theoretical principles of independence and sparse representation. In other words, the response spatial and chromatic properties of neurons in V1 can be accounted for by the redundancy-reduction hypothesis (Attneave 1954, Barlow 1961)

Some systematic differences between IC filters and V1 cells remain. Even the corrected filters shown in Figure 4d are still more chromaticity sensitive than V1 oriented cells (in the canonical view portrayed in Figure 2c, which disregards double-opponency), although they are not more so than non-oriented cells. Filters are also probably more double-opponent than simple cells. These differences are discussed below.

Limitations of the IC analysis

ICA is not a guaranteed method for finding an independent code for a data set. It is designed to discover independent sources of variability (basis functions), assuming

these are linearly superposed to form the observed data. Natural images break this assumption, because they are not formed by a linear superposition of sources (occlusion would be a better model than superposition). Under these circumstances, ICA can only discover sources that appear (by their non-Gaussianity) to be independent; these may be unrelated to the underlying structure of the data set.

Another limitation of our study is that the number of IC filters is capped by the dimensionality of the input data, which can artificially limit our ability to capture the structure of the input distribution. This limitation may become more critical as dimensionality increases, as when going from achromatic to chromatic images. Generating an overcomplete basis set (e.g. Olshausen and Field 1996; Lewicki and Sejnowski 2000) from colored natural scenes would likely change the distribution of spatial tuning, and may also change the distribution of color tuning.

Although we consider the effects of noise on neurophysiological experiments, we do not consider its effects on the redundancy-reduction hypothesis. Atick and Redlich (1990) have shown that, under noisy conditions, the receptive fields need to be more correlated (less independent), in order to preserve information about the image. We do not yet have an ICA model which allows us to take this into account.

Finally, ICA produces a strictly linear encoding; real neurons exhibit output nonlinearities and contrast normalization (e.g. Heeger 1992a, b), which are not part of our ICA model. There is evidence that nonlinearities play a role in V1 color processing (De Valois et al. 2000, Hanazawa et al. 2000). However, these nonlinearities primarily seem to sharpen a cell's tuning across color stimuli (De Valois et al. 2000). We surmise that

this kind of sharpening nonlinearity might enhance the effect of noise and separability bias in studies of V1.

Filters vs. basis functions

In order to compare the Independent Components of natural visual input with the receptive fields of real neurons, it is necessary to decide whether the IC filters or the IC basis functions are comparable to real receptive fields. For achromatic images, the basis functions and filters are very similar to one another, and this decision is not very significant (van Hateren and van der Schaaf 1998). For color data, however, there are substantial differences between the spatial and chromatic structure of the basis functions and filters (compare the color tuning of filters in Figure 2b to the equivalent basis functions in 2e), which makes the choice critical. There has been some disagreement about this question in the color ICA literature: Hoyer and Hyvärinen (2000) and Lee et al (2002) focus on basis functions, whilst Tailor et al. (2000) and Doi et al (2003) focus on filters.

The mathematical formulation of ICA is unambiguous that IC filters are the correct choice for comparison with neuronal receptive fields. Basis functions represent sources of variability in the data set; they are notional image patches that can be superposed to generate the data set. IC filters, on the other hand, are simply linear filters designed to extract information from the data set; in this way, they are completely compatible with the popular linear-filtering model of simple cells (e.g. Field 1987).

Retinal cone mosaic

There is a discrepancy between our results and those of Doi et al. (2003), who also analyzed LMS IC filters, but used a model featuring a fixed preprocessing stage mimicking the distribution of cones in the retinal mosaic. Their results, however, compare rather poorly to their choice of V1 data (Hanazawa et al. 2000), in both the prevalence of color selectivity (54% in V1 vs. 5% in their filters) and color tuning distribution (broad in V1 vs. extremely peaked in their filters).In addition, their model's retinogeniculate stage included many fewer S-preferring cells (~3%) than koniocellular/parvocellular LGN (~12%). The likely explanation for these differences is that Doi et al. only modeled the fovea (actually foveola), so that just 3% of the cone inputs to their model cortex were S-type. Most primate studies of color, including the data they use for comparison, were done in the perifovea, where the proportion of S cones is much higher: Lennie et al. (1990) studied cells within the central 3° of the visual field, and in fact Hanazawa et al.'s cells were between 0.8° and 2.4°. Within the central 2° (excluding the foveola), S cones represent at least 10% of the population (de Monasterio et al. 1985). Therefore, Doi et al.'s results may be most valid for minute foveolar RFs that are acutely sensitive to the structure of the cone mosaic.

Our present model, which assumes that S-cone density does not constrain RFs' spatial structure, compares better with existing physiological data. However, if the model were to incorporate a retinal mosaic stage with a normal perifoveal concentration of S cones, we would expect an increase in the proportion of luminance-preferring filters (given Doi et al.'s results), and possibly improvement in the fit between the model and V1.

Double-opponency and separability

An interesting feature of our IC filters is that the vast majority is double-opponent. This double-opponency has two components: first, each cone type's excitatory and inhibitory inputs balance across the RF; second, the inputs from opponent cones are exactly opposite in phase. The balance of excitatory and inhibitory inputs is a natural outcome for ICA, primarily because unbalanced filters would be correlated. The phase opponency, however, arises from a fixed property of the early visual system: the overlap in the absorption spectra of L and M cones, as well as S and M cones, forces the filters to decorrelate those input pairs as much as possible. The color statistics of natural scenes may also contribute significantly to opponency (Lee et al. 2002).

Double-opponency seemed rare in Lennie et al.'s study (1990). This is likely to be an underestimate because they used achromatic gratings to measure the optimal SF and orientation of the cells in their sample. This reflects an assumption of spatial-chromatic separability, and generates especially misleading results for double-opponent cells. Figure 7a shows a schematic double-opponent cell whose preferred stimulus contains a yellow-blue edge. When an achromatic grating (of optimal orientation and SF) is presented at any position, its light stripe will excite the yellow (L+M)and blue (S) inputs in one subfield equally, causing them to cancel out. Its dark stripe will do the same, and thus the response will not modulate. As a result, the estimates of preferred SF and orientation will be inaccurate; achromatic gratings cannot be used to estimate the tuning of double-opponent cells.

This effect can be demonstrated in our ICA data. An IC filter that responds poorly to achromatic gratings, much like the schematic cell in Figure 7a, is shown in Figure 7b.

Its true best color grating stimulus, which has the filter's dominant orientation and shows the influence of its yellow (L+M) and green (M) inputs, is shown in Figure 7c. However, if one assumes separability and stimulates this filter with an achromatic grating, the orientation and SF measurement is confounded by the double-opponency, and the resulting "best" grating (Figure 7d) bears no relation to the RF; it seems primarily influenced by spatial noise, and gives rise to arbitrary color tuning (with error shown by the open circle in Figure 4b).

More recent studies, using reverse correlation (Conway 2001) and cone-isolating stimuli (Johnson et al. 2001), have found a population of double-opponent cells. However, it is likely that the nearly obligatory double-opponency of our filters exceeds that of cortical cells. One possible reason is that the cortex, being subject to noise, does not decorrelate its receptive fields to the same degree as our noise-free IC filters. Another possible reason is that our image preprocessing excludes some known properties of the precortical visual system, such as chromatic aberration, the lower spatial resolution of the S-cone system, and the scattered color tuning of LGN cells. It may be that such considerations also help explain why our filters show magenta-green opponency rather than the red-cyan reported by Conway (2001).

Non-oriented cells

It has often been supposed that non-oriented cells in V1 are the substrate for color tuning, rather than oriented simple and complex cells (Hubel and Livingstone 1984). However, ICA generates few non-oriented, center-surround filters, because oriented features are more significant sources of variance in natural scenes than center-surround features. This would seem to make ICA a poor model for the center-surround color-selective cells in cytochrome oxidase blobs. However, we did find many small,

chromatically double-opponent filters, especially among the lower-variance ICs. These resemble the side-by-side double-opponent subunits found by Johnson et al. (2001) and the wide-band orientation tuned cells of Conway (2001), both of which probably occur in blobs. Also, consistent with the traditional understanding of blobs, we found that strength of chromaticity is inversely related to strength of orientation tuning. ICA might therefore be able to partially model color selectivity within blobs, however a complete model for V1 will require additional organizing principles such as topography (Barrow et al. 1996; Hyvärinen et al. 2001).

Conclusions

The similarity between the color independent components of natural scenes and receptive fields in V1 suggests that redundancy reduction (by ICA in particular) provides a plausible account of spatiochromatic receptive field structure in V1. This similarity is not apparent from inspection, largely because some filters that appear colored are often very sensitive to luminance variations. It is likely that a similar effect is present in V1, where simple cells are conventionally thought to be luminance-dominated, but we find that they are likely to have substantial color tuning that would be evident if their inputs were visualized.

We predict that, as our understanding of V1 color coding improves, the color sensitivity of oriented cells will assume a more important role. In place of a clear division between luminance and color coding, our results suggest that simple cells may multiplex spatial and color information. Similarly, our results highlight the importance of double-opponency, which is advantageous for coding of colored borders and, as we have shown, for redundancy reduction. Finally, the success of ICA in accounting for

spatiochromatic receptive field structure in V1 suggests that redundancy reduction will also prove to be a fruitful hypothesis in other sensory systems.

Acknowledgments

The authors are grateful to C. Alejandro Párraga, Gavin Brelstaff, Tom Troscianko and Ian Moorhead for making their “hyperspectral” natural scenes publicly available, and to C. Alejandro Párraga for the Nikon camera sensitivity curves. We thank Mark Kvale and Christina Onufryk for helpful commentary. This research was begun while MSC was supported by a Frank Knox Fellowship to the University of Cambridge, and was continued with support from an NDSEG Fellowship. BW was supported by a BBSRC studentship.

References

Atick JJ, and Redlich AN. Towards a theory of early visual processing. *Neural Comput*, 2:308-320, 1990.

Attneave F. Some informational aspects of visual perception. *Psych Rev* 61: 183-193, 1954.

Barlow HB. Sensory mechanisms, the reduction of redundancy, and intelligence. In: *The Mechanisation of Thought Processes*. London: HM Stationery Office, 1959.

Barlow HB. Unsupervised Learning. *Neural Comput* 1: 295-311, 1989.

Barrow HG, Bray AJ, and Budd JM. A self-organizing model of "color blob" formation. *Neural Comput* 8: 1427-1448, 1996.

Baylor DA, Nunn BJ, and Schnapf JL. Spectral sensitivity of cones of the monkey Macaca fascicularis. *J Physiol* 390: 145-160, 1987.

Bell AJ, and Sejnowski TJ. The "independent components" of natural scenes are edge filters. *Vis Res* 37: 3327-3338, 1997.

Comon P. Independent Component Analysis—a new concept? *Signal Processing* 36: 287-314, 1994.

Conway BR. Spatial structure of cone inputs to color cells in alert macaque primary visual cortex (V-1). *J Neurosci* 21: 2768-2783, 2001.

Derrington AM, Krauskopf J, and Lennie P. Chromatic mechanisms in lateral geniculate nucleus of macaque. *J Physiol* 357: 241-265, 1984.

de Monasterio FM, McCrane EP, Newlander JK, and Schein SJ. Density profile of blue-sensitive cones along the horizontal meridian of macaque retina. *Invest Opth Vis Sci* 26: 289-302, 1985.

De Valois RL, Albrecht DG, and Thorell LG. Spatial frequency selectivity of cells in macaque visual cortex. *Vis Res* 22: 545-559, 1982.

De Valois RL, Cottaris NP, Elfar SD, Mahon LE, and Wilson JA. Some transformations of color information from lateral geniculate nucleus to striate cortex. Proc Natl Acad Sci USA 97: 4997-5002, 2000.

Doi E, Inui T, Lee TW, Wachtler T, and Sejnowski TJ. Spatiochromatic receptive field properties derived from information-theoretic analyses of cone mosaic responses to natural scenes. *Neural Comput* 15: 397-417, 2003.

Field DJ, and Tolhurst DJ. The structure and symmetry of simple-cell receptive-field profiles in the cat's visual cortex. *Proc R Soc London B* 228: 379-400, 1986.

Field DJ. Relations between the statistics of natural images and the response properties of cortical cells. *J Opt Soc Am A* 4: 2379-2394, 1987.

Field DJ. What is the goal of sensory coding? *Neural Comput* 6: 559-601, 1994.

Fisher NI, Lewis T, and Embleton BJJ. *Statistical analysis of spherical data*. Cambridge, UK: Cambridge University Press, 1987.

Hanazawa A, Komatsu H, and Murakami I. Neural selectivity for hue and saturation of colour in the primary visual cortex of the monkey. *Eur J Neurosci* 12: 1753-1763, 2000.

Heeger DJ. Normalization of cell responses in cat striate cortex. Vis Neurosci 9:181-97, 1992a.

Heeger DJ. Half-squaring in responses of cat striate cells. Vis Neurosci 9:427-43, 1992b.

Hoyer PO, and Hyvärinen A. Independent component analysis applied to feature extraction from colour and stereo images. *Network* 11: 191-210, 2000.

Hubel DH, and Wiesel TN. Receptive fields and functional architecture of monkey striate cortex. *J Physiol* 195: 215-243, 1968.

Hyvärinen A, Hoyer PO, and Inki M. Topographic independent component analysis. *Neural Comput* 13: 1527-1558, 2001.

Johnson EN, Hawken MJ, and Shapley R. The spatial transformation of color in the primary visual cortex of the macaque monkey. *Nature Neurosci* 4: 409-416, 2001.

Lee TW, Wachtler T, and Sejnowski TJ. Color opponency is an efficient representation of spectral properties in natural scenes. *Vis Res* 42: 2095-2103, 2002.

Lennie P, Krauskopf J, and Sclar G. Chromatic mechanisms in striate cortex of macaque. *J Neurosci* 10: 649-669, 1990.

Levine MW. Variability of responses to sinusoidal modulation. *Vis Neurosci* 11: 155-163, 1994.

Lewicki MS and Sejnowski TJ. Learning overcomplete representations. *Neural Comput* 12: 337-365, 2000.

Livingstone MS, and Hubel DH. Anatomy and physiology of a color system in the primate visual cortex. *J Neurosci* 4: 309-356, 1984.

MacLeod DI, and Boynton RM. Chromaticity diagram showing cone excitation by stimuli of equal luminance. *J Opt Soc Am* 69: 1183-1186, 1979.

Makeig S et al. EEGLAB: ICA Toolbox for Psychophysiological Research [Online]. Computational Neurobiology Laboratory, The Salk Institute for Biological Studies. www.sccn.ucsd.edu/~scott/ica.html [2002].

Michael CR. Color vision mechanisms in monkey striate cortex: simple cells with dual opponent-color receptive fields. *J Neurophys* 41: 1233-1249, 1978.

Olshausen BA, and Field DJ. Emergence of simple-cell receptive field properties by learning a sparse code for natural images. *Nature* 381: 607-609, 1996.

Parker AJ, and Hawken MJ. Two-dimensional spatial structure of receptive fields in monkey striate cortex. *J Opt Soc Am A* 5: 598-605, 1988.

Párraga CA, Brelstaff G, Troscianko T, and Moorhead IR. Color and luminance information in natural scenes. *J Opt Soc Am A* 15: 563-569, 1998.

Ringach DL. Spatial structure and symmetry of simple-cell receptive fields in macaque primary visual cortex. *J Neurophysiol* 88: 455-463, 2002.

Ringach DL, Shapley RM, and Hawken MJ. Orientation selectivity in macaque V1: diversity and laminar dependence. *J Neurosci* 22:5639-5651, 2002.

Ruderman DL, Cronin TW, and Chiao C. Statistics of cone responses to natural images: implications for visual coding. *J Opt Soc Am A* 15: 2036-2045, 1998.

Smith VC, and Pokorny J. Spectral sensitivity of the foveal cone photopigments between 400 and 500 nm. *Vis Res* 15: 161-171, 1975.

Tailor DR, Finkel LH, and Buchsbaum G. Color-opponent receptive fields derived from independent component analysis of natural images. *Vis Res* 40: 2671-2676, 2000.

van Hateren JH, and Ruderman DL. Independent component analysis of natural image sequences yields spatio-temporal filters similar to simple cells in primary visual cortex. *Proc R Soc London B* 265: 2315-2320, 1998.

van Hateren JH, and van der Schaaf A. Independent component filters of natural images compared with simple cells in primary visual cortex. *Proc R Soc London B* 265: 359-366, 1998.

Wachtler T, Lee TW, and Sejnowski TJ. Chromatic structure of natural scenes. *J Opt Soc Am A* 18: 65-77, 2001.

Willmore B, Watters PA, and Tolhurst DJ. A comparison of natural-image-based models of simple-cell coding. *Perception* 29:1017-1040, 2000.

Figure Legends

Figure 1. Sample of IC filters and IC basis functions generated by running ICA on differently encoded input, and RGB and LMS absorption spectra used in encoding

ICs, which contain positive- and negative-valued pixels with arbitrary range, were normalized so that a value of 0 is displayed as medium intensity (0.5) and all pixels of an IC are between 0 and 1. (a-b) IC filters generated from RGB input (a), and from JPEG-encoded RGB input (b). Filters were manually separated into approximate color opponency type (blue-yellow vs. red-green). Within color groups, they are subdivided by spatial structure (full-field, Gabor-like, checkerboard (present in (b) only), and small noisy patches. Finally, within these groups, they are arranged in descending order by variance. (c) IC filters generated from images encoded using human LMS cone sensitivities, shown in pseudocolor so that L is red, M green, and S blue. LMS filters are divided into two groups (short vertical white line): significant and artifactual, using the criteria of van Hateren and van der Schaaf (1998). Within groups, they are shown in decreasing order by variance. (d) LMS IC basis functions, matched to the filters in (c). (e) Absorption spectra of human L, M and S cones. (f) R, G and B absorption spectra of a typical digital camera.

Figure 2. The color tuning of IC filters and V1 cells is similar

The color tuning of each IC (a, b, e) was measured in the DKL colorspace following the methods of Lennie et al. (1990), except that we optimized the grating stimulus over all

spatial and chromatic gratings (the “ideal case”). The color tuning of V1 cells (c,d) is replotted from Lennie et al., and assumes that spatial and chromatic tuning are separable, with separate stages for finding the optimal achromatic and chromatic stimuli. Each plot’s marginal distributions indicate density, as a percentage of the total distribution. (a) IC filters derived from RGB input and transformed into the LMS cone space. (b) LMS filters. (c) Oriented cells. (d) Non-oriented cells. (e) IC basis functions from LMS filters. Following Lennie et al., azimuth is plotted between -45° and 135° to better depict clustering near 0°, and is taken modulo 180° to emphasize color opponency rather than exact color preference.

Figure 3. Spatial tuning parameters of LMS IC filters resemble achromatic ICs and simple cells

The spatial properties of each IC were measured using each IC’s best achromatic stimulus. White bars are the distributions for all ICs; gray bars are the distribution of ICs that were non-artifactual by van Hateren and van der Schaaf (1998)’s criteria. Solid circles and lines show the reported V1 distributions (De Valois et al. 1982, Parker and Hawken 1988), and open circles and dashed lines show the achromatic IC distributions (van Hateren and van der Schaaf 1998). (a) best orientation; 0º corresponds to vertical. (b) bandwidth (full width at half maximum) of orientation tuning. (c) best spatial frequency, (d) bandwidth of spatial frequency tuning, (e) aspect ratio of the RF envelope.

Figure 4. Experimental biases strongly affect the comparison between ICs and physiological data, but correction greatly improves the correspondence with V1

Three sources of bias were considered: low variance artifactual ICs, the assumption of spatial-chromatic separability, and physiological noise. (a) Color tuning (plotted as in Figure 2) of the LMS filters that were artifactual according to van Hateren and van der Schaaf's (1998) criteria. Marginal distributions indicate density, as a percentage of the total distribution. (b) Bias in physiological color tuning data due to assuming separability, inferred from comparing measurements of filter color tuning made under ideal and experimental conditions. The open circle represents the example in Figure 7. (c) Bias due to physiological noise. The displacement shown is between the mean of 25 color tuning estimates and the ideal tuning. (d) Distribution of LMS IC filters after all biases—artifactual ICs, separability, and noise—are taken into account. Marginal distributions are as in (a).

Figure 5. Width of orientation tuning correlates with preference for chromaticity

Color tuning elevation, measured with optimal chromatic gratings, is shown as a function of orientation tuning bandwidth. Solid circles: non-artifactual LMS IC filters. Open circles: artifactual filters.

Figure 6. LMS IC filter responses to cone-isolating gratings fall into distinct double-opponent groups

LMS IC filter responses were measured in each color plane, using cone-isolating gratings, and the spatial relationship between cone inputs was determined. (a) Response amplitudes of each filter to its optimal L, M and S-isolating gratings (open circles). Dots indicate the projections of the open circles onto the cardinal (L=0, M=0, S=0) planes;

near (0,0,0) the open circles are superimposed on the projection dots. Axes are in arbitrary units; the L and M axes are much greater in magnitude than the S axis because of the overlapping absorption spectra of L and M cones. In order to make those two dimensions independent, the filter must be stronger along those axes. (b-e) Phase difference between the optimal cone-isolating gratings for pairs of cones. A peak at 180° indicates phase opponency, while a peak at 0° indicates phase coherence. Among the strongly L- and M-sensitive filters, (b) shows the phase difference between M and L, and (c) the difference between M and S. Among the strongly S-sensitive filters, (d) shows the phase difference between S and M, and (e) the difference between S and L.

Figure 7. Assuming separability may cause severe biases when measuring double-opponent cells

The problem with assuming separability of spatial and chromatic RFs is illustrated, schematically and with an example IC filter. For clarity, we describe stimuli using RGB terms, even though the filter is LMS-encoded. (a) Schematic double-opponent cell with four subfields. The leftmost subfield is inhibited by red, and the rightmost is excited by green. The middle two subfields are yellow-blue double-opponent; the middle left subfield is excited by red and green (R+ and G+) and inhibited by blue (B-) while the middle right is inhibited by red and green (R- and G-) and excited by blue (B+).(b) A filter from our data set (open circle in figure 4b) which is modeled by the schematic cell. It is shown in full color (left), and then separated into color planes for clarity (right). In all figures, medium gray indicates zero input. (c) The true best cone-opponent grating. Note that it is spatially aligned with the filter and shows the influence of its L and M cone

inputs. (d) False “best” cone-opponent grating, assuming spatial-chromatic separability. Note that the grating is completely misaligned and shows little evidence of the filter’s strong L input.

Table 1. Normalized Kullback-Leibler distances between color tuning distributions of V1 cells and IC filters

	IC group					
Cell class	Raw	Non-artifactual	Separability corrected	Noise corrected	Separability + Noise	All corrections
Oriented	1.02	0.84	0.88	0.89	0.72	0.58
Non-oriented	0.88	0.79	0.84	0.64	0.50	0.48
Pool of both	0.79	0.66	0.71	0.59	0.44	0.37

All distances are normalized relative to the Kullback-Leibler distance between oriented and non-oriented cell classes (see Methods). "Pool of both" contains both oriented and non-oriented cells. "All corrections" indicates that high variance ICs have been corrected for both separability and noise.

Figure 1

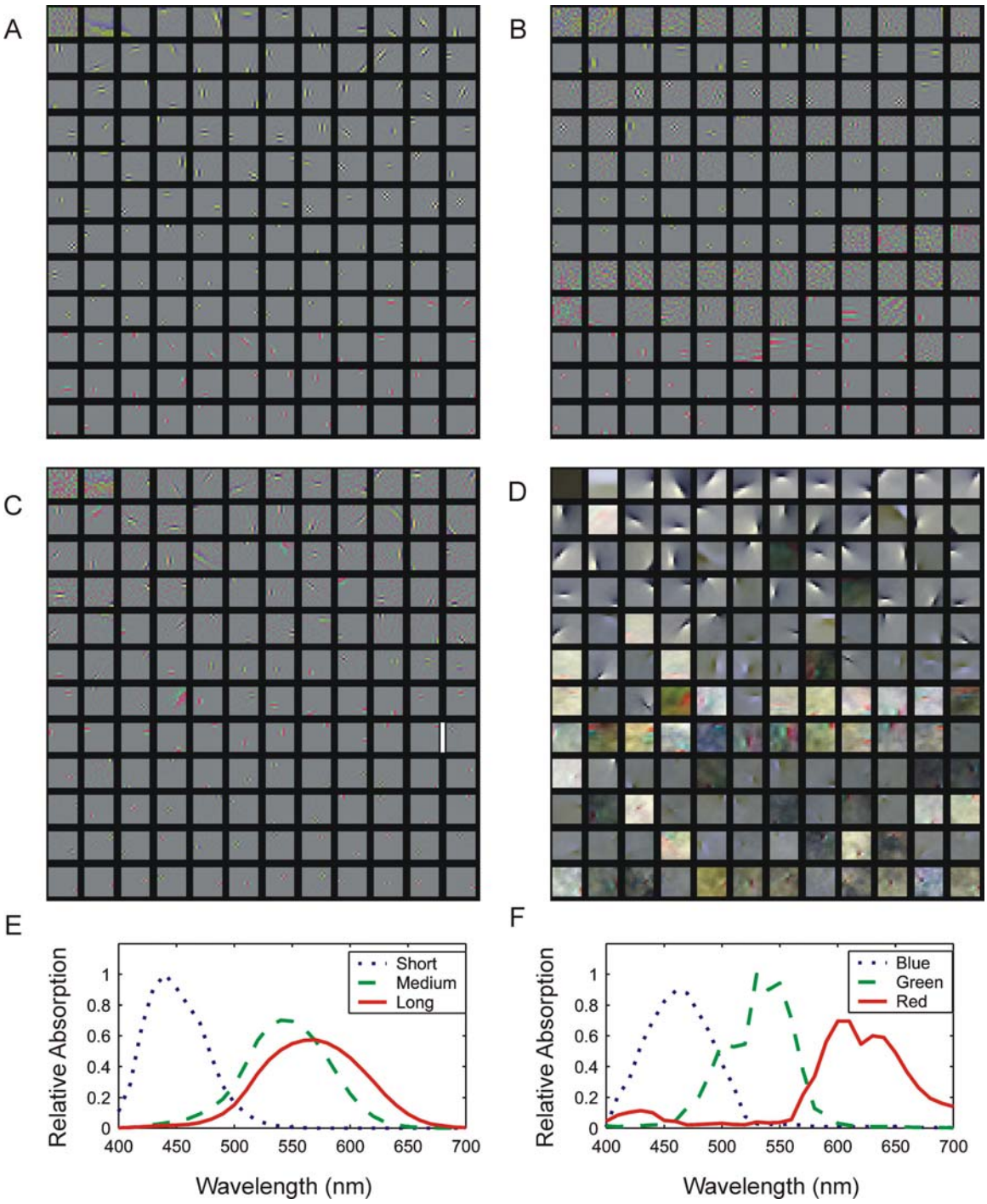
A
B
C
D
E
F
Relative Absorption
Short
Medium
Long
Wavelength (nm)
Blue
Green
Red

Figure 2

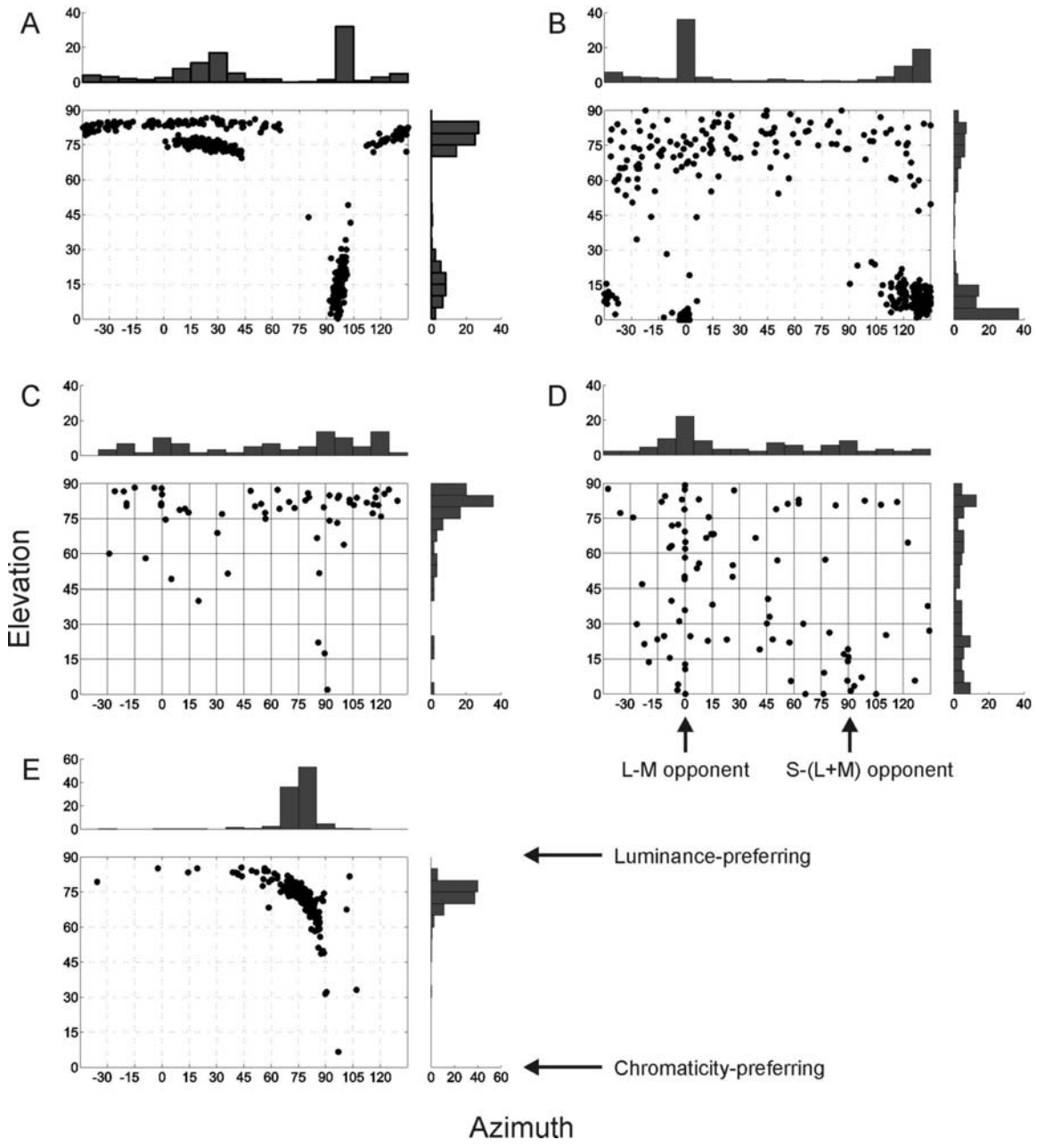
A
B
C
D
E
Elevation
Azimuth
L-M opponent
S-(L+M) opponent
Luminance-preferring
Chromaticity-preferring

Figure 3

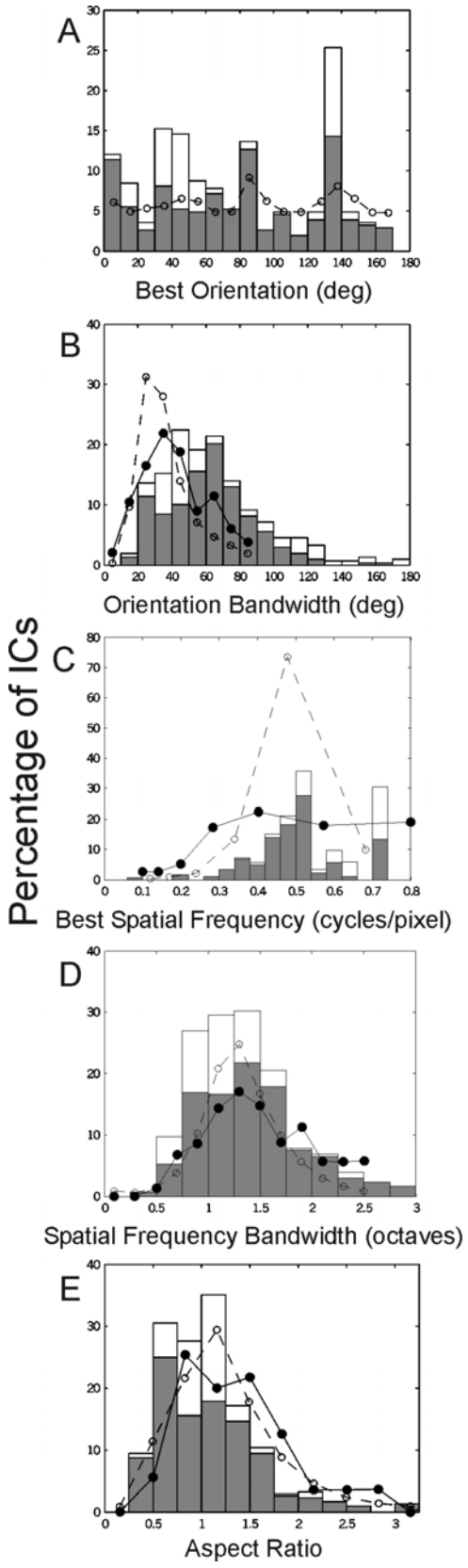
A
Best Orientation (deg)
B
Orientation Bandwidth (deg)
Percentage of ICs
C
Best Spatial Frequency (cycles/pixel)
D
Spatial Frequency Bandwidth (octaves)
E
Aspect Ratio

Figure 4

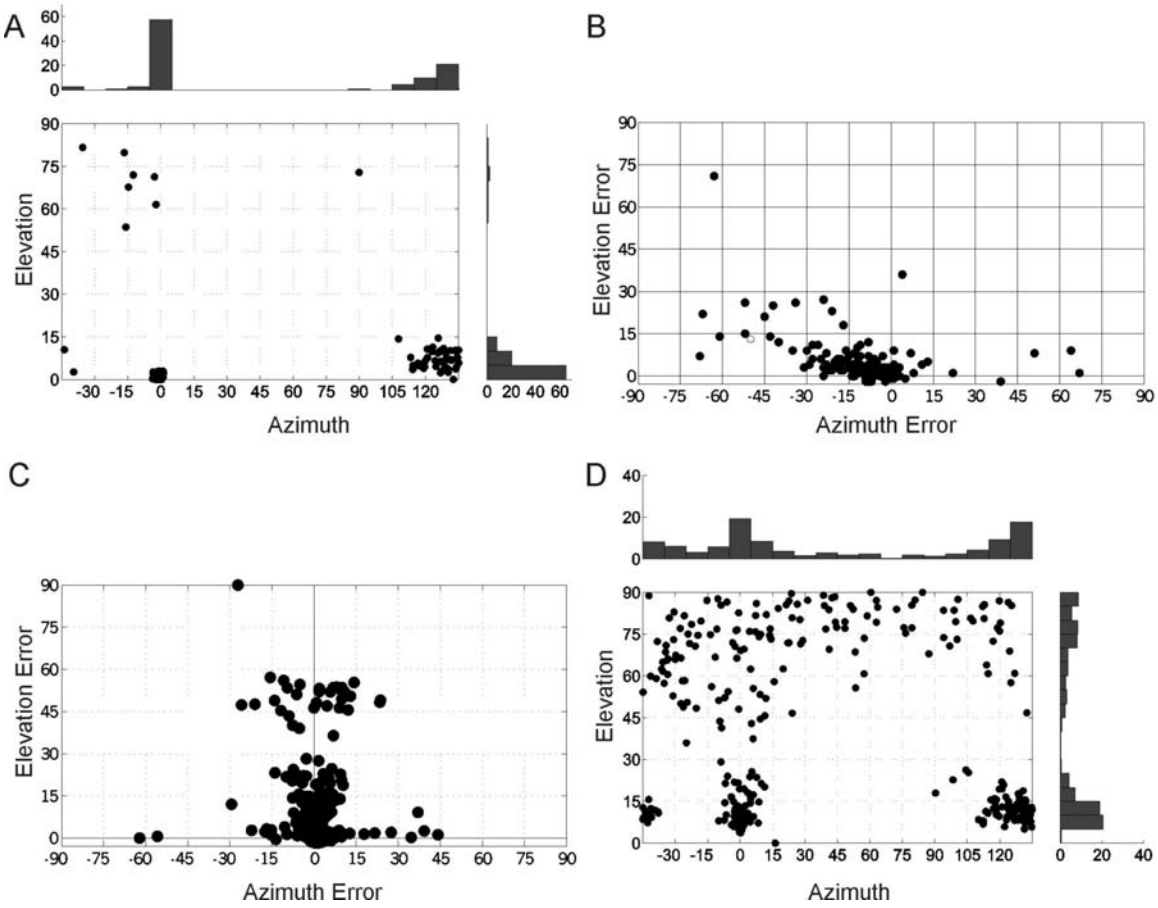
A
B
C
D
Elevation
Azimuth
Elevation Error
Azimuth Error
Elevation
Azimuth

Figure 5

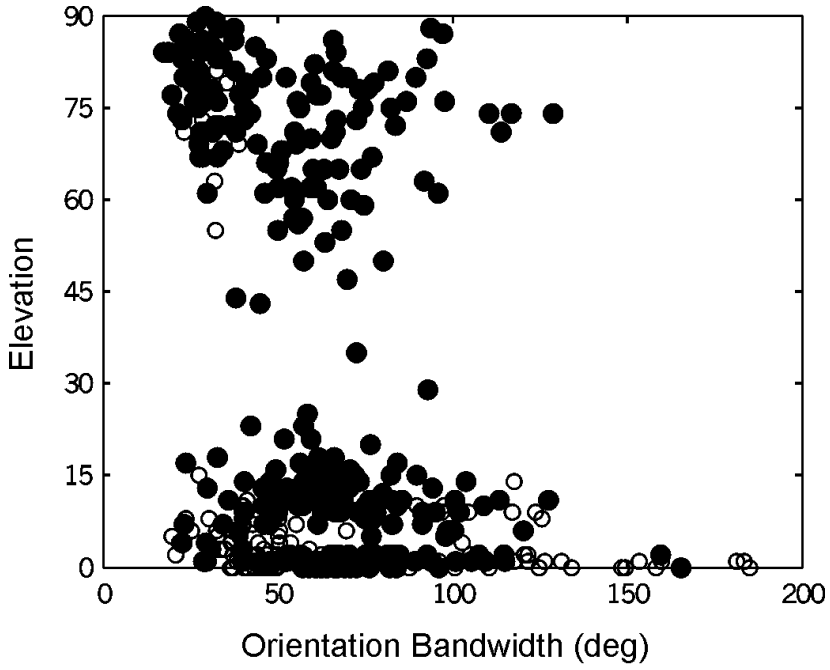
90
75
60
45
30
15
0
Elevation
0
50
100
150
200
Orientation Bandwidth (deg)

Figure 6

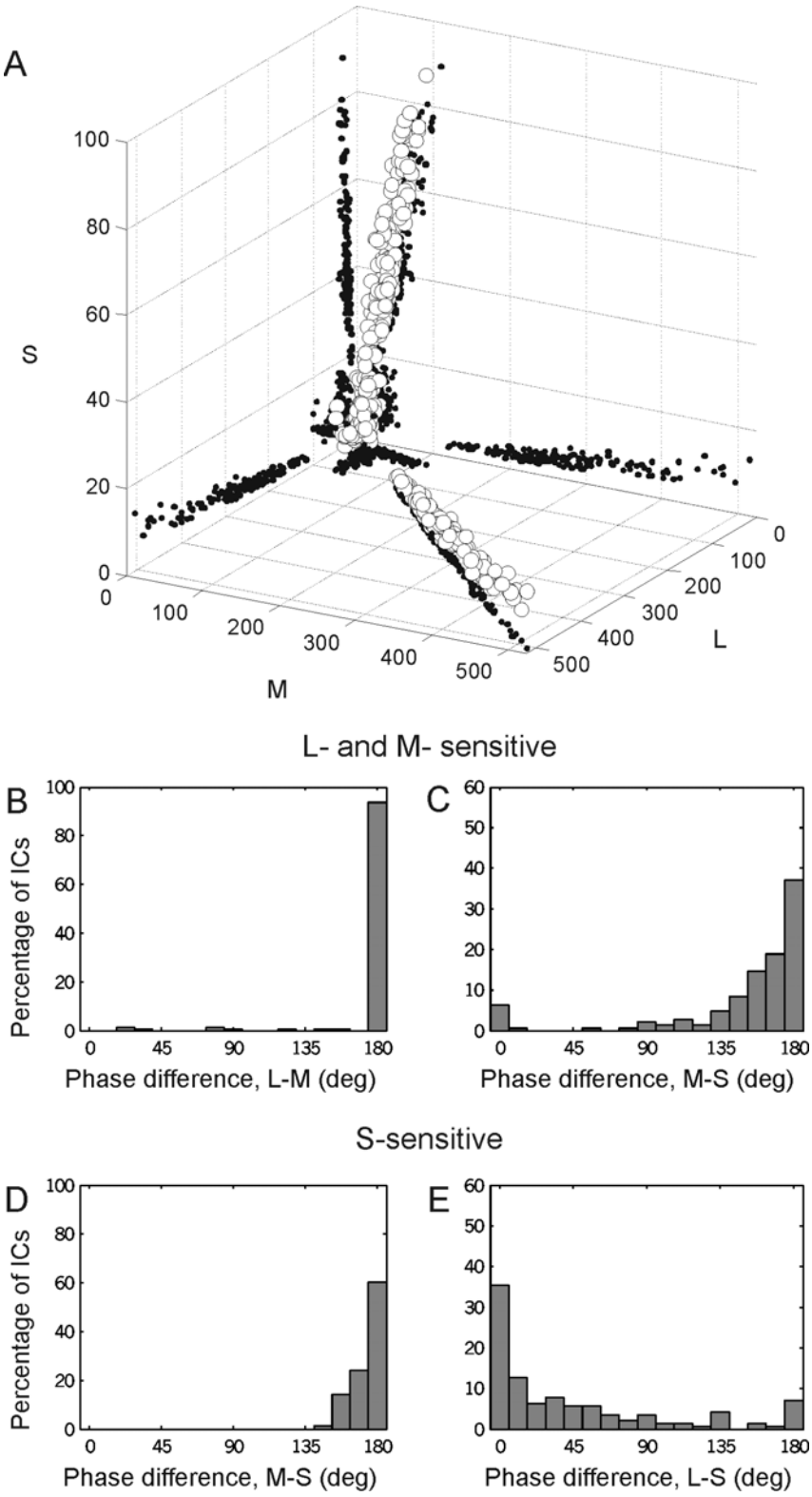
A
S
M
L
L- and M- sensitive
B
C
Percentage of ICs
Phase difference, L-M (deg)
Phase difference, M-S (deg)
S-sensitive
D
E
Percentage of ICs
Phase difference, M-S (deg)
Phase difference, L-S (deg)

Figure 7